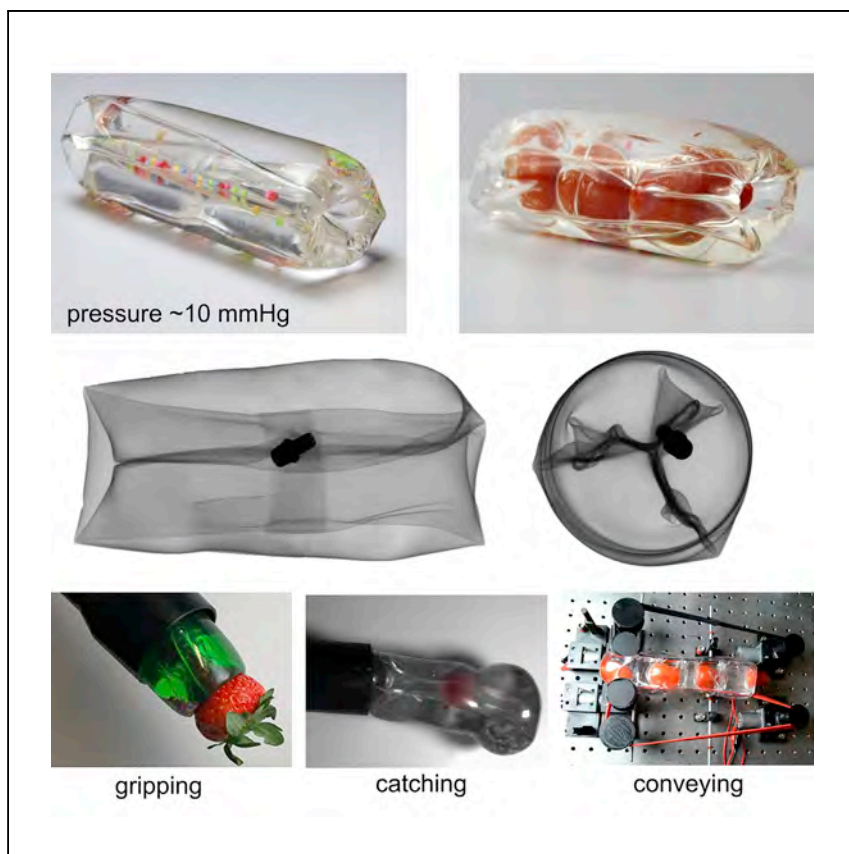


Article

Bio-inspired design of soft mechanisms using a toroidal hydrostat



To mimic the biological functions of gripping, catching, and conveying, Root et al. design three soft mechanisms using a toroidal hydrostat. These mechanisms leverage the inversions and eversions of a tubular, toroidal membrane inflated with a fluid. These demonstrations suggest that inflatable, topological structures of polymer films provide a versatile approach for engineering soft robotic devices.

Samuel E. Root, Daniel J. Preston, Gideon O. Feifke, ..., Markus P. Nemitz, Jovanna A. Tracz, George M. Whitesides
gmwhitesides@gmwgroup.harvard.edu

Highlights

Bio-inspired mechanisms using the topology of soft structures pressurized with fluid

A gripping mechanism (~ 10 mmHg, ~ 10 N) based on the inversion of an inflated tube

A catching mechanism (≈ 400 m/s²) based on a catapulting inversion

A conveying mechanism (~ 1 cm/s) based upon a continuous inversion and eversion process

Article

Bio-inspired design of soft mechanisms using a toroidal hydrostat

Samuel E. Root,^{1,2} Daniel J. Preston,¹ Gideon O. Feifke,¹ Hunter Wallace,¹ Renz Marion Alcoran,¹ Markus P. Nemitz,¹ Jovanna A. Tracz,¹ and George M. Whitesides^{1,*}

SUMMARY

Biology is replete with soft mechanisms of potential use for robotics. Here, we report that a soft, toroidal hydrostat can be used to perform three functions found in both living and engineered systems: gripping, catching, and conveying. We demonstrate a gripping mechanism that uses a tubular inversion to encapsulate objects within a crumpled elastic membrane under hydrostatic pressure. This mechanism produces gripping forces that depend predictably upon the geometric and materials properties of the system. We next demonstrate a catching mechanism akin to that of a chameleon's tongue: the elasticity of the membrane is used to power a catapulting inversion process ($\approx 400 \text{ m/s}^2$) to capture flying objects (e.g., a bouncing ball). Finally, we demonstrate a conveying mechanism that passes objects through the center of the toroidal tube ($\sim 1 \text{ cm/s}$) using a continuous inversion-eversion process. The hybrid hard-soft mechanisms presented here can be applied toward the integration of soft functionality into robotic systems.

INTRODUCTION

Hard robots face difficulty when manipulating delicate, irregularly, or variably shaped objects.¹ While existing soft robotic grippers have made progress, actuation remains a concern. Pneumatically driven soft robots require compressed air, and electrically driven soft robots require high voltages. Simple soft components that can be actuated at low voltages (5–12 V) would allow for the straightforward design of hybrid systems. Moreover, it is of general interest to identify ways in which biological functions, such as locomotion, capturing objects (e.g., for predation), and internal transport of objects (e.g., for digestion), can be simply mimicked and built into robotic systems using soft materials and actuators.² In particular, the soft mechanisms for gripping, catching, and conveying (Figure 1) presented in this work were inspired by (1) the *proboscis*, an eversible, tubular organ that various worms (e.g., bloodworms) use for burrowing into sand, catching prey, and excreting digested food,^{3–5} and (2) the chameleon's tongue, a soft catapulting system for rapidly catching moving prey several body lengths away.^{6,7}

Over the last half century, hard robots have become increasingly effective at performing repetitive tasks in tightly controlled environments, such as assembly lines. The “real world,” however, is rarely as predictable. The unstructured nature of our environment makes gripping and manipulating variably and irregularly shaped objects a particularly problematic task for robots.¹ An important development for robotic gripping was the idea that compliant materials could be used

¹Department of Chemistry and Chemical Biology, Harvard University, 12 Oxford Street, Cambridge, MA 02138, USA

²Lead contact

*Correspondence: gmwhitesides@gmwgroup.harvard.edu
<https://doi.org/10.1016/j.xcrp.2021.100572>



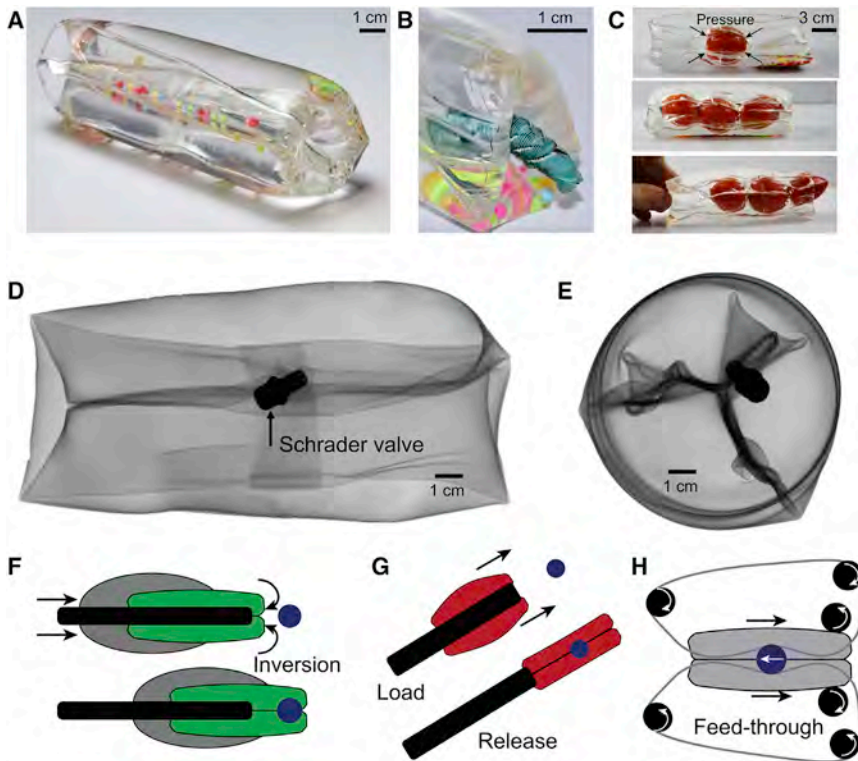


Figure 1. A soft, toroidal hydrostat

(A) Photograph of a commercially available toroidal hydrostat filled with water (this version, sold as a children’s toy, also contains colorful beads). The length of this toroidal, soft-polymer hydrostat is 12.5 cm, and the diameter is 3.75 cm.

(B) Photograph shows the soft toroid inverting around a live hornworm, without harming it.

(C) Photographs show the toroid encapsulating small tomatoes under uniform hydrostatic pressure. Manual application of pressure to one side drives (e.g., pinching) an inversion-eversion process that can take in, expel, or transport objects.

(D–H) X-ray absorption photographs show the internal structure of a toroidal hydrostat filled with air from (D) a longitudinal view and (E) an axial view. Schematic drawings of mechanisms for (F) gripping an object through inversion and encapsulation, (G) catching an object by releasing loaded elastic energy, and (H) a continuous feed-through process driven by rotary motors and belts.

to reduce the complexity of control required for gripping irregularly shaped, fragile objects.^{8,9} Over the years, numerous soft gripping systems have been devised.⁸ These grippers can be broadly classified by one of three gripping mechanisms: (1) mechanical actuation, (2) controlled stiffness, and (3) controlled adhesion.⁸

Soft grippers based upon fluidic elastomer actuators^{9–12} have advanced to the point of industrial use—they are one of the most commercially useful products to have emerged from the field of soft robotics. Grippers have also been made using a loosely packed bladder of granular media (a semi-fluid), which conforms to the surface of an object and provides a strong gripping force upon pulling a vacuum and “jamming” the granules.¹³ Festo AG & Co. has demonstrated that a vacuum-actuated, inverting soft bladder filled with fluid could provide an adaptable gripping solution.¹⁴ These approaches require a pneumatic energy source to function. While pneumatic actuation is feasible in cases where pressure sources are readily available, other applications would benefit from soft robotic functionality using a power source that does not rely on pneumatic pressure, such as electrical power sources.

Examples of electrically powered soft grippers include electroactive polymers, such as dielectric elastomer actuators¹⁵ (DEAs). DEAs can exhibit high actuation strains (>100%),¹⁶ operate at high efficiency (80%), are self-sensing,¹⁷ and can be made to be transparent.¹⁸ They require, however, high voltages (~kV) and are prone to failure from dielectric breakdown and aging.¹⁹ Moreover, it is difficult to scale up the forces exerted by these actuators because large areas are required and stacked actuators are more likely to experience electrical failure. Recently, Keplinger and co-workers described a new class of soft actuators that circumvent some of the stability and stacking issues associated with DEAs by employing a liquid dielectric.^{20,21} Such actuators were used to construct grippers; however, these grippers still required high voltages (~kV) to function.

In both Festo's¹⁴ and Keplinger's^{20,21} gripping demonstrations, the key innovation was the use of a fluid encapsulated within an elastomeric membrane. This approach is analogous to a biological hydrostat, such as a jellyfish. The gripper invented by Festo is particularly reminiscent of a chameleon's tongue, a powerful predatory tool that enables these predators to catch insects. Inverting a hydrostatically pressurized, elastic membrane around an object provides a strong gripping force with an evenly distributed contact pressure. While the ability to pick and place delicate objects in an automated fashion is of undeniable commercial importance, there may be some instances in which a continuous transportation mechanism is preferable (e.g., a conveyor belt). In biology, peristalsis has evolved as a mechanism for internal transportation. Tubular organs, such as the esophagus, employ radially symmetric contractions and relaxations of muscle that propagate like a wave to propel boluses of food along the digestive tract.²² Such biological principles have inspired the design of analogous soft peristaltic pumping systems, powered by pneumatics.²³ Although peristaltic motion is effective for transporting lubricated objects, it is not effective for dry objects where friction impedes the motion. For such a case, it would be preferable for the interior walls of the tube to move along with the object being transported.

Hawkes et al. recently demonstrated a useful approach for soft robotic locomotion that employed the pneumatic eversion of a tubular membrane to navigate environments, mimicking a growth mechanism reminiscent of vines.²⁴ Moreover, the inversion and eversion process of a toroidal hydrostat (Figures 1A–1C, commercially available as a children's toy, called a "water wiggly") has previously been proposed as a method of robotic locomotion.²⁵ These prior works suggested to us that inflated topological structures capable of inverting and everting could be of more general use for imparting soft robotic functionality.

In this article, we demonstrate how a toroidal hydrostat can perform three biologically inspired robotic functions: gripping, catching, and conveying (Figure 1). This unique elasto-fluidic object can invert around, encapsulate, and grip irregularly shaped objects within an elastomeric membrane under a uniform hydrostatic pressure. Moreover, the inherent rubber elasticity of the toroidal hydrostat can be leveraged to store mechanical energy and drive a catapult mechanism for rapidly catching objects. Finally, the toroidal topology of the hydrostat enables a novel feed-through transportation mechanism that represents a hybrid between biological peristalsis and a man-made conveyor belt. The soft mechanisms we present here could be used for the robotic automation of agricultural processes and biological research. More generally, the use of polymer films arranged into non-trivial, inflatable topologies offers the potential for the development of new actuation mechanisms in soft robots.²⁶

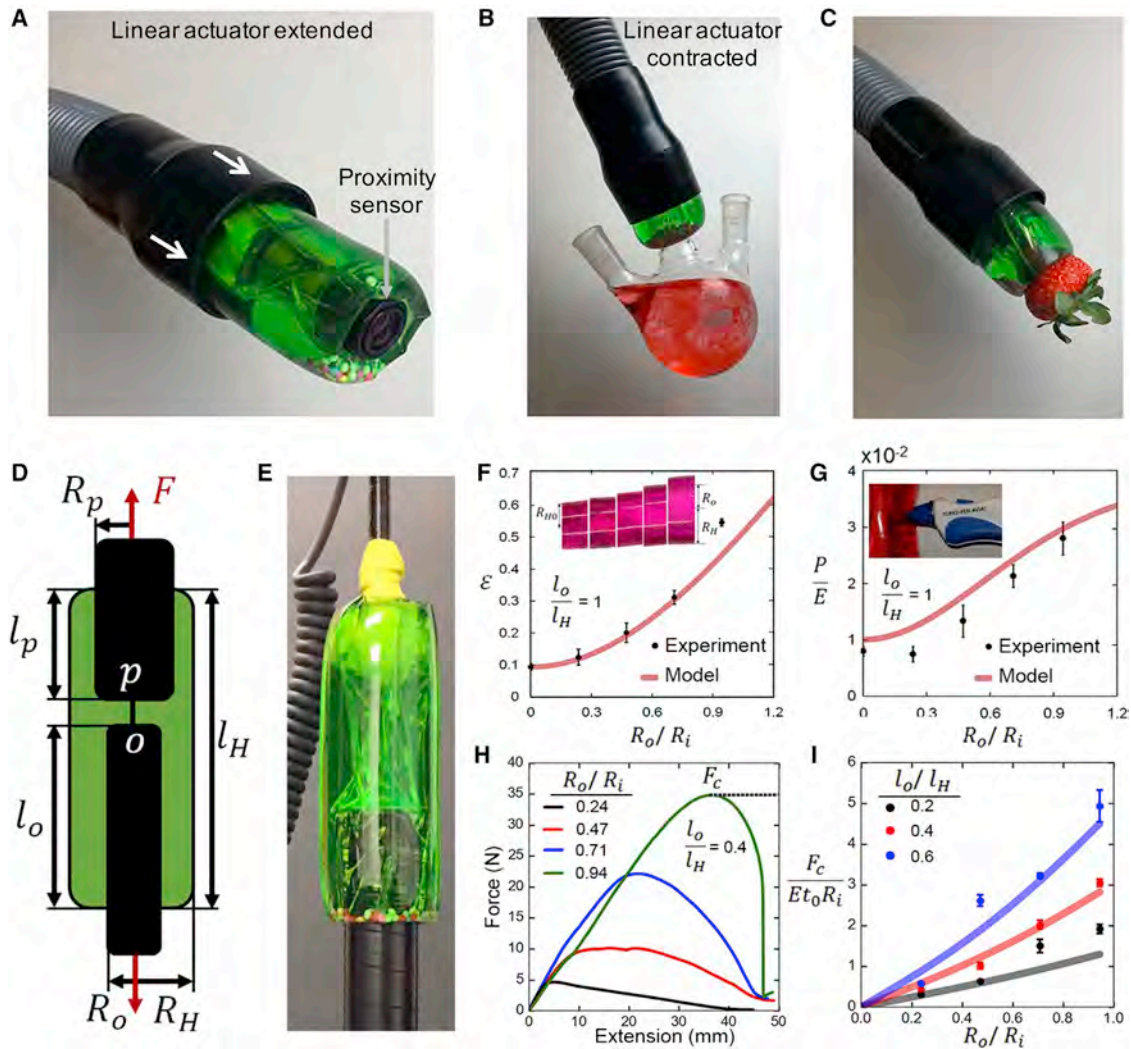


Figure 2. Gripping with a toroidal hydrostat

(A–C) A photograph of (A) the electronic gripping device constructed from the toroidal hydrostat, (B) the device picking up a three-necked flask, and (C) the device picking up a ripe strawberry.

(D) A free-body diagram showing the geometrical configuration of the pull-testing experiments used to measure the gripping mechanics.

(E) Photograph of experimental pull-testing setup (Instron).

(F and G) Comparison of model predictions and experimental measurements for (F) circumferential strain and (G) Laplace pressure buildup due to the insertion of a rod of varying radius. Insets show photographs of the experiments. (E) Load versus displacement curves obtained from pull-tests of cylinders of constant encapsulated length and varied radii. (F) Comparison of model predictions with experiment for the dimensionless critical gripping force versus dimensionless radius of the encapsulated cylinder for various encapsulated lengths. Error bars represent the standard deviation of 7 measurements.

RESULTS

Gripping

We first constructed a hybrid soft-hard device that gently encapsulates and grips various irregularly shaped, fragile objects (Figures 2A–2C). The device contains an outer cylinder (in this case, a flexible vacuum tube) that couples the exterior of the toroidal hydrostat to the motion of the internal, linear servo motor. When the internal linear servo is extended, the outer cylinder pulls back on the toroidal hydrostat, and it everts at the tip. When the internal linear servo is retracted, the outer cylinder pushes forward and the toroidal hydrostat inverts to encapsulate

objects positioned in front of it. Some features of this specific implementation include that it (1) is constructed of low-cost, commercially available components, (2) operates at $\approx 5\text{--}12\text{ V}$, (3) contains a low-cost infrared photoelectric proximity sensor that can be used to detect objects in front of the gripper and initiate actuation, (4) can pick up $>1\text{ kg}$, and (5) has fast actuation times ($\sim 1\text{ s}$). For most of our demonstrations, we used the “water wiggly,” a commercially available children’s toy, to make our results simple to reproduce (Figures 1A–1C). Fabrication of a toroidal hydrostat is simple, however, and described in the [Experimental Procedures](#). Figures 1D and 1E show X-ray absorption photographs of our custom-made, silicone toroidal hydrostat inflated with air.

We note that, during the preparation of this manuscript, similar gripping devices were reported by two separate groups.^{27,28} For gripping, the only advantage the toroidal topology provides in comparison to Festo’s vacuum-actuated hydrostatic inversion gripper¹⁴ is the ability to put a sensor (or a camera) directly at the front of the gripper (Figure 2A). The placement of the linear actuator and sensor within the soft gripper, however, adds weight to the robotic appendage and renders it not entirely soft, which is disadvantageous compared to a pneumatically actuated end-effector. Regardless of actuation mechanism (pneumatic versus electromechanical), to design robotic grippers for specific applications it is useful to have a model for the gripping mechanics of such a hydrostatic inversion process, including a quantitative description of the pressures and forces involved.

Gripping mechanics

We developed a simple mathematical model (Note S1) to describe the mechanics of the gripper and experimentally investigated how the material properties of the toroidal hydrostat influence the forces exerted while gripping objects of varied geometries (Figures 2D–2I). To simplify the analysis, we consider an idealized cylindrical geometry shown in Figures 2D and 2E. Definitions of geometric variables are given in Figure 2D. All measurements were performed with the commercially available “water wiggly” and 3D-printed acrylonitrile butadiene styrene (ABS) rods. The following assumptions were used in the derivation of the model: (1) Coulomb friction, (2) cylindrical Laplace pressure, (3) linear elasticity of the membrane, and (4) conservation of volume. We expect these assumptions to provide the most accurate approximation in the limit that the radius of the object is much less than the radius of the toroidal tube, $R_o/R_i \ll 1$.

We first measured the radial expansion of the hydrostat with cylindrical objects of varied radius inserted (Figure 2F). Radial expansion was measured by wrapping a piece of tape around the circumference of the toroid and then peeling it off and measuring the length. A cylindrical, incompressible, hydrostatic model predicts the following behavior for radial strain, ε , under the experimental conditions ($l_o/l_H = 1$):

$$\varepsilon = \sqrt{\left(\frac{R_{H0}}{R_i}\right)^2 + \left(\frac{R_o}{R_i}\right)^2} - 1. \quad (\text{Equation 1})$$

Here, R_{H0} is the radius of the unperturbed “water wiggly,” R_i is the radius of the tube in the unstrained state (i.e., after draining the water). We observed excellent agreement between the model and experiments (Figure 2F) in the case where $R_o/R_i < 1$; however, when $R_o/R_i \sim 1$ the model fails. This failure is likely due to the loss of validity of the assumptions of (1) a cylindrical geometry and (2) linear elastic deformation. Experimentally, we observed that in this limit the tube assumes an ellipsoidal shape described by two radii of curvature.

We next measured the increase in Laplace pressure of the hydrostat with cylindrical objects of varied radii inserted. Laplace pressure was measured using a tonometer: a precise medical device for measuring intraocular pressure (Figure 2G). Our model predicts the following behavior for the hydrostatic Laplace pressure, P , under the experimental conditions ($l_0/l_H = 1$):

$$\frac{P}{E} = \frac{\epsilon t_0 R_i}{R_{H0}^2 + R_0^2}, \quad (\text{Equation 2})$$

where E is the tensile modulus of the membrane and was measured to be 2 MPa by pull-testing experiments (Figure S4). We observed close agreement between the model and experiments (Figure 2G); however, we suspect some slight systematic error in the measurement, as the tonometer is calibrated specifically for the measurement of intraocular pressure.

Force versus extension curves were measured for encapsulated rods of varied length and radii using a universal Instron pull-tester (Figures 2E and 2H). The critical gripping force was extracted as the peak of the force trace. The dimensionless critical gripping force predicted from our model can be written as:

$$\frac{F_C}{Et_0 R_i} = 2\pi\mu R_0 l_0 \left(\frac{1}{R_i R_H} - \frac{1}{R_H^2} \right). \quad (\text{Equation 3})$$

Here, t_0 is initial the thickness of the elastic membrane in the unstrained state. The predictions of this equation are compared to experimental measurements in Figure 2I. The validity of this model was assessed by using the coefficient of friction as the sole fitting parameter for a multivariable (l_0/l , R_0/R_i) non-linear regression and then comparing the optimized value ($\mu = 0.94$) to the value measured independently using a friction sled experiment ($\mu = 0.91$) (see Note S2, Figure S3). The agreement between this minimalistic model with experimental measurements is remarkable given that many of the assumptions underlying the model are imperfect. The model could be further refined by considering the axial strain of the hydrostat, non-linear elasticity of the membrane, non-cylindrical curvature, and the role of gravity on hydrostatic pressure. Moreover, modifications would be needed to account for the compressibility of an air-filled toroidal hydrostat. Nevertheless, this simple model could be used for the design of gripping devices with tailored mechanics for specific applications that require either strong or gentle gripping pressures and forces.

Catching

The chameleon's tongue can project forward with more power than any known muscle.^{5,6} This power is enabled by a unique biomechanical catapult system comprising a stiff cartilage frame for aiming the projection, nested sheaths of collagen for storing elastic energy, and a radially contracting accelerator muscle for supplying the mechanical energy.^{5,6} When the tongue launches, the collagen sheaths relax at the tip of the cartilage, driving a "sliding-spring" mechanism that converts potential energy into kinetic energy. To replicate this mechanism with the toroidal hydrostat, we loaded it onto a rod (a pipe made of polyvinyl chloride, PVC) with a radius comparable to that of the hydrostat (4.8 cm). We adhered the toroid to the tip of the rod by jamming a ping pong ball such that it pinched a small section of the membrane against the inner wall of the PVC pipe (Figure 3A). When the toroid was loaded onto the rod, it bulged in the middle and formed an ellipsoidal shape due to a buildup of hydrostatic pressure. When the toroid was released, the stored elastic energy projected the toroid off the tip of the rod in a rapidly accelerating inversion

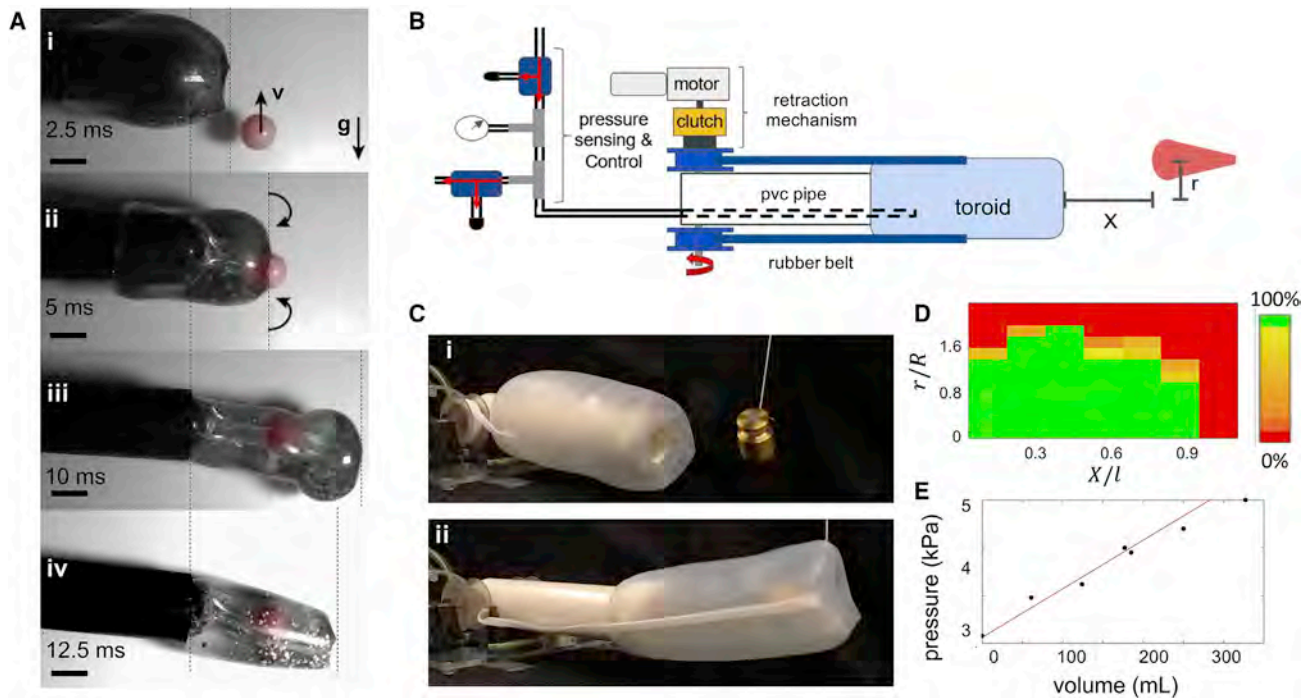


Figure 3. Catching with a catapulting toroidal hydrostat

(A) Snapshots taken from a high-speed video recording of the catching process for a water-filled toroidal hydrostat showing (A,i) the initial release, (A,ii) contact with the rubber ball, (A,iii) the fully engulfed rubber ball, and (A,iv) the final resting state. The rubber ball was colored red for clarity. The scale bar represents 2.5 cm.

(B) A schematic diagram showing the components of the automated catapulting catching device.

(C) Photographs of the device (C,i) loaded with an object swinging in front of it and (C,ii) engulfing the object.

(D) A heatmap showing the range over which the device can successfully capture objects.

(E) A plot showing the linear relationship between the pressure of the toroidal hydrostat after it has engulfed an object and the volume of the object.

process that acted to catch and swallow small objects in front of the tip, e.g., a bouncing rubber ball (Figure 3A; Video S1).

To substantiate our observations, we recorded high-speed videos of the catching process and analyzed the frames to determine the position and the velocity of the tip as a function of time. Analysis of the video (Figure S5) yields an acceleration of 400 m s^{-2} , an acceleration, of similar magnitude to a chameleon's tongue ($500\text{--}2500 \text{ m s}^{-2}$)

Once the chameleon's tongue has captured its prey, the tongue is retracted with a contractile muscle.^{5,6} To demonstrate the incorporation of such a catapulting-retraction mechanism into an automated robotic system, we constructed the hybrid hard-soft device shown in Figures 3B and 3C. The soft component of the robotic system comprised an air-filled, silicone toroid with rubber belts on the exterior to allow for the automated retraction of the toroid onto a rod. We employed an air-filled toroid so that we could easily control the pressure within it using pneumatic equipment (valves, pressure sensor, and a source of compressed air) and because we expected the reduced inertia and viscosity of the gas relative to a liquid to facilitate a more rapid acceleration. The device was controlled electronically using an Arduino Uno microcontroller. The sensing required for automated control was implemented through an electronic pressure sensor coupled to the toroid through a tube. The pressure inside the toroid was controlled using the electronic valves, pressure

source, and vent shown schematically in [Figure 3B](#). Automated retraction was implemented using a gear motor coupled to an electromagnetic clutch and a spindle for drawing the belt. When the clutch was engaged and the motor was powered, the toroid was retracted onto the rod. The state of the toroid was monitored through the pressure increase and retraction was halted at a critical value, determined empirically and dependent upon the initial pressurization of the toroid. When the magnetic clutch was released, the toroid accelerated rapidly along the axis of the rod to encapsulate objects in front of it. While testing our device, we noted two surprising and useful features.

First, the toroid was capable of catching objects that were not positioned directly in its path, i.e., objects with positional uncertainty. We quantified this observation by placing a spheroidal object at various positions relative to the toroid, defined by the x , R axes shown in [Figure 3B](#), and then empirically determining the probability of successfully inverting around the object as a function of position, using 7 trials for each position. The heatmap shown in [Figure 3D](#) shows that the toroid could capture objects with an axial offset, r , larger than its radius, R . To capture such objects, the toroid curls around them. This curling motion is caused by the asymmetry induced upon frictional contact with an object to be captured. The capture range depends upon a variety of variables including the modulus and frictional behavior, as well as the geometry of the toroid and the object being captured.

Second, the increase in pressure within the toroid upon capture of an object depended linearly upon the volume of the object. Thus, the pressure change provides a simple way of inferring the volume of objects that have been captured. Such a functionality is quite useful, as volume is difficult to estimate visually (without a known geometric model) and can be used as a quantity for sorting objects for a variety of agricultural, industrial, or scientific purposes.

Conveying

We next demonstrated a feed-through process, in which the unique motion of the toroidal hydrostats allows for the continuous collection and transportation of objects ([Figures 4A–4E](#); [Video S2](#)). The continuous inversion process is driven by the rotary motion of four electrical motors. Two of the motors drive rubber belts through the interior of the toroid, while the other two provide a counterbalancing traction force to the exterior of the toroid. We found that rollers with concave shapes proved the most uniform traction forces. The directions of motion are shown schematically in [Figure 4C](#). The result is a dynamic process that functions to transport objects through the interior of the toroid. The softness of the transportation process was demonstrated by passing ripe tomatoes through the center of the device ([Figure 4E](#)). In this preliminary prototype, the transportation speed is approximately 1.3 cm/s.

DISCUSSION

We demonstrated that a toroidal hydrostat acts as a soft mechanical transducer with unique and useful behavior that is easily integrated with hard robotic components to add soft robotic functionality. The gripping mechanism presented provides uniformly distributed, easily controlled pressures and forces based on the principle of hydrostatic inversion. In a practical implementation, machine vision and robotic control algorithms could be integrated with this gripper to implement it in a general way.

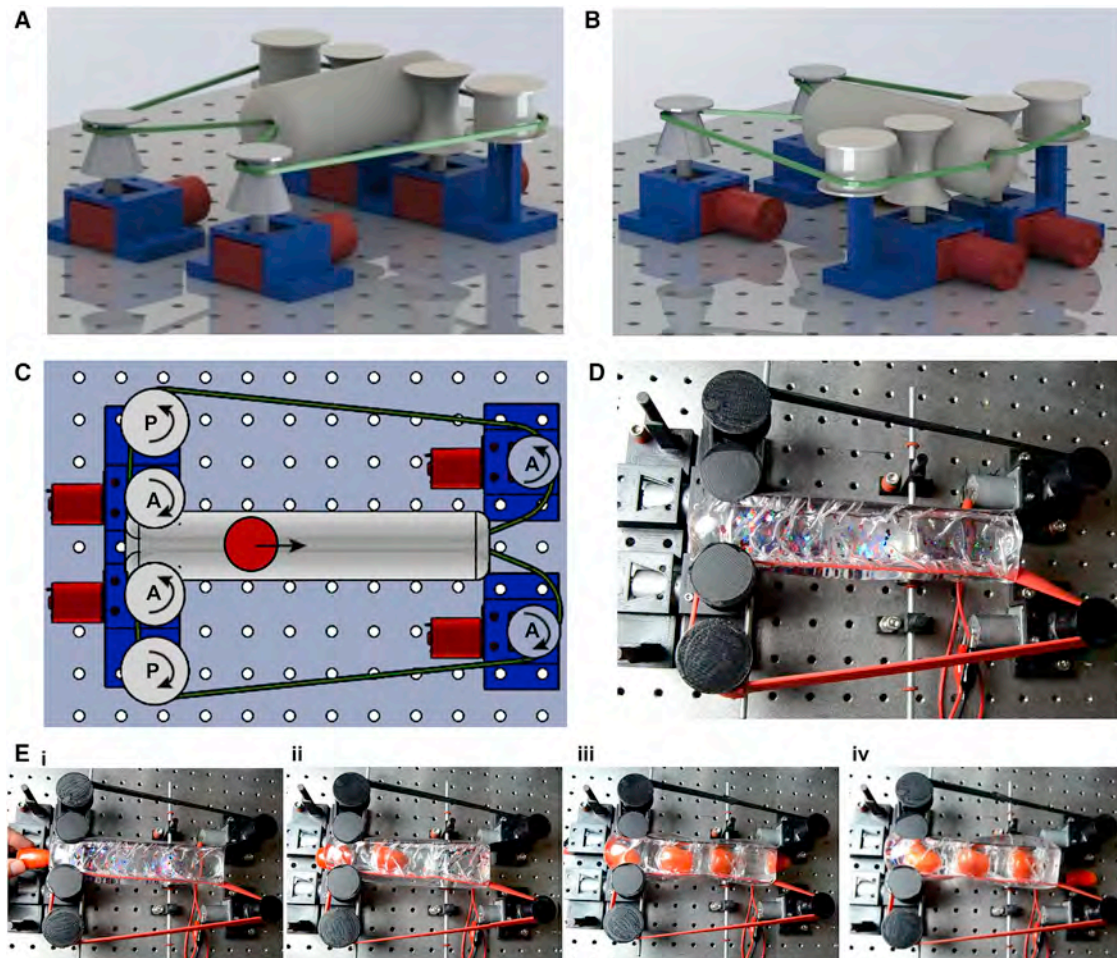


Figure 4. Conveying with a toroidal hydrostat

(A) Computer rendering showing the conveying device at an angle from the front.

(B) Computer rendering showing the conveying device at an angle from the back.

(C) Computer rendering of the hydrostatic conveying device from a top-down view. A represents an active roller driven by a motor, and P represents a passive roller with a ball bearing. Arrows indicate the direction of motion.

(D) Photograph of the constructed device from a top-down view.

(E) Photographs of the device inverting around, engulfing, and expelling tomatoes. For scale, threaded holes on the breadboard are spaced one inch apart.

This approach could find use in automation problems that require the gripping and transportation of delicate objects. Potential users include (1) biological researchers interested in automating experimental studies that require the transfer and manipulation of small animals, like insects, mice, worms, or fish, and (2) farmers interested in automating the harvest of delicate fruits and vegetables. This technology faces two primary drawbacks: (1) this inversion mechanism only works to pick up an object if some part of it can fit inside the toroidal tube (it does not work as well as Festo's hydrostatic inversion gripper¹⁴ to grip onto flat objects using a suction force because of the crumples in the inverted elastic membrane, nor is it possible to grip objects that are much larger than the toroid orifice); and (2) the tube can be punctured by sharp objects—broken glass, for instance—leading the pressurized fluid to leak out.

The device implementation of the catching mechanism has the potential to be improved upon further. For example, the rod used for aiming the gripper could be made using a soft or variable stiffness pneumatic actuator with the capability of both controlling the direction of the catapult launch, and radially inflating as a mechanism to load mechanical energy into the attached toroidal compartment. It may also be possible to design a pneumatic retraction mechanism to make the entire device soft.

The device implementation of the conveying mechanism has the potential to be expanded upon and optimized. One issue with the current system is asymmetry due to the presence of a seam where the ends of a tube are adhered to form a toroid. This asymmetry causes periodic irregularity in the continuous inversion process. This problem could be mitigated with longer tubes, a flexible instead of a stretchable membrane, and an improved sealing process to reduce inhomogeneities in the stiffness of the tube. It would also be of interest to either connect several conveyers in series to change the direction of transportation or configure a single, longer toroidal tube in a bended conformation. The ability to dynamically manipulate the conveying path would make this process particularly attractive for sorting processes.

Overall, this work demonstrates how elastofluidic mechanisms inspired by nature can be simply implemented with hybrid hard-soft robotic systems to develop new and interesting functionality, and how non-trivial topology can be used to impart new functions to inflatable soft robotic systems.

EXPERIMENTAL PROCEDURES

Resource availability

Lead contact

Requests for further information can be directed to and will be fulfilled by lead contact, Sam Root (samroot.phd@gmail.com).

Materials availability

This study did not generate any new or unique materials.

Data and code availability

This study did not generate a dataset, raw experimental data and code for analysis is available by request from the lead contact.

Fabrication of inflatable silicone toroid

A device to fabricate a silicone tube was constructed by mounting a PVC pipe in a horizontal orientation and rotating it with a DC motor (Figure S1A). Three coatings of liquid silicone (SORTA-Clear 12) were applied to the rotating cylinder by slowly (over the course of several minutes) pouring a total amount of 0.7 g of liquid silicone per square inch of surface area such that none of it dripped off. A silicone paint brush was used to manually spread the viscous silicone liquid to make a uniform coating, which was allowed to cure for 2 h prior to applying the subsequent coatings. After the silicone coating was fully cured, the end pieces were cut off with a razor blade and the tube was rolled off the PVC pipe (Figure S1B). One end of the tube was manually inverted, bringing the two ends together (Figure S1C). For the air-filled toroid, the inner end of the tube was subsequently stretched onto a PVC pipe, and a coating of Momentive RTV159 Silicone Adhesive Sealant was applied with a margin of overlap of 1 cm. Finally, the outer end of the tube was flipped and brought into contact with the sealant and held in place with rubber bands while the sealant

cured. During this time, a Schrader valve was inserted into the gap between the two endpoints and more silicone adhesive was applied to seal it. After the adhesive cured, the toroid was inflated, as shown in Figure S2. For the water-filled toroid, a slightly different procedure was applied in which the water was inserted prior to sealing (Figure S1D) and held out of the way by twisting the tube (Figure S1E)

Mechanical measurements

The coefficient of friction of the thermoplastic elastomer membrane of the water wiggly was measured using a friction sled rig (Figure S3A). The membrane was laminated onto a wood surface using double-sided tape on the backside and duct tape around the edges. A sled of the same 3D-printed Nylon used for the gripping force measurements was loaded with weights and attached to the load cell of an Instron universal testing machine by means of a nylon string pulley to measure the dynamic frictional force (Figure S3B) as a function of the normal force (the steady-state value at a displacement rate of 50 mm/s) and obtain the coefficient of friction through linear regression (Figure S3C). As shown in Figure S3D, the coefficient of friction measured this way matched well with the best fit of the gripping model.

The gripping force was measured using an Instron universal testing machine. The force sensor was connected to a rod with a diameter of 1 cm that was wrapped with a layer of yellow sealant tape (Fiberglast, 580). The toroid was everted and inverted onto the tacky rod and remained adhesively stuck in that position for the duration of the experiments. The toroid was pushed up on the top rod and then back down onto the bottom rod to configure the system shown in Figure 2E, with the bottom 3D-printed acrylonitrile butadiene styrene (ABS) rods clamped to the base of the Instron. The top rod was pulled upward at a rate of 50 mm/s, and the force was measured as a function of displacement. The critical gripping force was taken as the maximum value of the force obtained before the rod was released.

SUPPLEMENTAL INFORMATION

Supplemental information can be found online at <https://doi.org/10.1016/j.xcrp.2021.100572>.

ACKNOWLEDGMENTS

This research was funded by the Department of Energy award #DE-SC0000989 and Department of Energy, Office of Basic Energy Science, Division of Materials Science and Engineering, award ER45852. J.A.T. acknowledges the Wyss Institute for Biologically Inspired Engineering at Harvard for salary support. R.M.A. acknowledges the REU program funded by NSF 1420570. We thank Professor L. Mahadevan for useful discussions related to the gripping model. We thank Dr. Derek Feifke for assisting with measurements of pressure by ocular tonometry.

AUTHOR CONTRIBUTIONS

S.E.R. conceptualized the project. S.E.R., D.J.P., G.O.F., H.W., and M.P.N. designed the experiments and demonstrations; S.E.R., D.J.P., G.O.F., H.W., R.M.A., M.P.N., and J.A.T. conducted the experiments and constructed the demonstrations. S.E.R., D.J.P., and G.O.W. wrote the manuscript. G.M.W. supervised the project and provided critical feedback on the experimental design, selection of demonstrations, and the writing of the manuscript.

DECLARATION OF INTERESTS

G.M.W. acknowledges an equity interest and board position in Soft Robotics Inc. All other authors declare that they have no competing interests.

Received: July 21, 2021

Revised: August 12, 2021

Accepted: August 20, 2021

Published: September 10, 2021

REFERENCES

- Hodson, R. (2018). How robots are grasping the art of gripping. *Nature* 557, S23–S25.
- Rajappan, A., Jumet, B., and Preston, D.J. (2021). Pneumatic soft robots take a step toward autonomy. *Sci. Robot.* 6, 1–3.
- Ockelmann, K.W., and Vahl, O. (1970). On the Biology of the Polychaete *Glycera Alba*, Especially Its Burrowing and Feeding. *Ophelia* 8, 275–294.
- Murphy, E.A.K., and Dorgan, K.M. (2011). Burrow extension with a proboscis: mechanics of burrowing by the glycerid *Hemipodus simplex*. *J. Exp. Biol.* 214, 1017–1027.
- Lichtenegger, H.C., Schöberl, T., Bartl, M.H., Waite, H., and Stucky, G.D. (2002). High abrasion resistance with sparse mineralization: copper biomineral in worm jaws. *Science* 298, 389–392.
- de Groot, J.H., and van Leeuwen, J.L. (2004). Evidence for an elastic projection mechanism in the chameleon tongue. *Proc. Biol. Sci.* 271, 761–770.
- Müller, U.K., and Kranenbarg, S. (2004). Physiology. Power at the tip of the tongue. *Science* 304, 217–219.
- Shintake, J., Cacucciolo, V., Floreano, D., and Shea, H. (2018). Soft Robotic Grippers. *Adv. Mater.* 1707035, e1707035.
- Ilievski, F., Mazzeo, A.D., Shepherd, R.F., Chen, X., and Whitesides, G.M. (2011). Soft robotics for chemists. *Angew. Chem. Int. Ed. Engl.* 50, 1890–1895.
- Suzumori, K., Iikura, S., and Tanaka, H. (1991). Development of Flexible Microactuator and Its Applications to Robotic Mechanisms. Proceedings of 1991 IEEE International Conference on Robotics and Automation, 1622–1627. <https://doi.org/10.1109/ROBOT.1991.131850>.
- Marchese, A.D., and Rus, D. (2016). Design, Kinematics, and Control of a Soft Spatial Fluidic Elastomer Manipulator. *Int. J. Robot. Res.* 35, 840–869.
- Wall, V., Zoller, G., and Brock, O. (2017). A Method for Sensorizing Soft Actuators and Its Application to the RBO Hand 2. Proceedings of the 2017 IEEE International Conference on Robotics and Automation (ICRA), 4965–4970. <https://doi.org/10.1109/ICRA.2017.7989577>.
- Brown, E., Rodenberg, N., Amend, J., Mozeika, A., Steltz, E., Zakin, M.R., Lipson, H., and Jaeger, H.M. (2010). Universal Robotic Gripper Based on the Jamming of Granular Material. *Proc. Natl. Acad. Sci. USA* 107, 18809–18814.
- Vogel, J., Höppner, H., and Weitschat, R. (2016). Robotic gripper and method for operating the same. Priority number: WO2017134092A1, Applicants: FESTO AG & CO KG, Filed February 2, 2016, and published August 10, 2017.
- Hajiesmaili, E., and Clarke, D.R. (2021). Dielectric Elastomer Actuators. *J. Appl. Phys.* 129, 151102.
- Pelrine, R., Kornbluh, R., Pei, Q., and Joseph, J. (2000). High-speed electrically actuated elastomers with strain greater than 100%. *Science* 287, 836–839.
- Keplinger, C., Kaltenbrunner, M., Arnold, N., and Bauer, S. (2008). Capacitive Extensometry for Transient Strain Analysis of Dielectric Elastomer Actuators. *Appl. Phys. Lett.* 92, 1–4.
- Keplinger, C., Sun, J.Y., Foo, C.C., Rothemund, P., Whitesides, G.M., and Suo, Z. (2013). Stretchable, transparent, ionic conductors. *Science* 341, 984–987.
- Brochu, P., and Pei, Q. (2010). Advances in dielectric elastomers for actuators and artificial muscles. *Macromol. Rapid Commun.* 31, 10–36.
- Kellaris, N., Gopaluni Venkata, V., Smith, G.M., Mitchell, S.K., and Keplinger, C. (2018). Peano-HASEL actuators: Muscle-mimetic, electrohydraulic transducers that linearly contract on activation. *Sci. Robot.* 3, 1–11.
- Acome, E., Mitchell, S.K., Morrissey, T.G., Emmett, M.B., Benjamin, C., King, M., Radakovitz, M., and Keplinger, C. (2018). Hydraulically amplified self-healing electrostatic actuators with muscle-like performance. *Science* 359, 61–65.
- Clavé, P., and Shaker, R. (2015). Dysphagia: current reality and scope of the problem. *Nat. Rev. Gastroenterol. Hepatol.* 12, 259–270.
- Chen, F.J., Dirven, S., Xu, W.L., and Li, X.N. (2014). Soft Actuator Mimicking Human Esophageal Peristalsis for a Swallowing Robot. *IEEE/ASME Trans. Mechatron.* 19, 1300–1308.
- Hawkes, E.W., Blumenschein, L.H., Greer, J.D., and Okamura, A.M. (2017). A soft robot that navigates its environment through growth. *Sci. Robot.* 2, 1–8.
- Orekhov, V., Yim, M., and Hong, D. (2010). Mechanics of a fluid filled everting toroidal robot for propulsion and going through a hole. Proceedings of the ASME 2010 International Design Engineering Technical Conferences and Computers and Information in Engineering Conference. 2, 1205–1212.
- Hawkes, E.W., Majidi, C., and Tolley, M.T. (2021). Hard questions for soft robotics. *Sci. Robot.* 6, 1–6.
- Li, H., Yao, J., Liu, C., Zhou, P., Xu, Y., and Zhao, Y. (2020). A Bioinspired Soft Swallowing Robot Based on Compliant Guiding Structure. *Soft Robot.* 7, 491–499.
- Zang, H., Liao, B., Lang, X., Zhao, Z.L., Yuan, W., and Feng, X.Q. (2020). Bionic Torus as a Self-Adaptive Soft Grasper in Robots. *Appl. Phys. Lett.* 116, 20–23.